

Supplementary Information for

CD8⁺ tissue-resident memory T cells promote liver fibrosis resolution by inducing apoptosis of hepatic stellate cells

Yuzo Koda,^{1,2} Toshiaki Teratani,¹ Po-Sung Chu,¹ Yuya Hagiwara,¹ Yohei Mikami,¹ Yosuke Harada,¹ Hanako Tsujikawa,³ Kentaro Miyamoto,¹ Takahiro Suzuki,¹ Nobuhito Taniki,¹ Tomohisa Sujino,¹ Michiie Sakamoto,³ Takanori Kanai,^{1,4*} Nobuhiro Nakamoto^{1*}

¹Division of Gastroenterology and Hepatology, Department of Internal Medicine, Keio University School of Medicine, Tokyo, Japan

²Mitsubishi Tanabe Pharma Corporation, Kanagawa, Japan

³Department of Pathology, Keio University School of Medicine, Tokyo, Japan

⁴Japan Agency for Medical Research and Development, AMED, Tokyo, Japan

*Address correspondence to Nobuhiro Nakamoto (nobuhiro@z2.keio.jp) and Takanori Kanai (takagast@z2.keio.jp), Division of Gastroenterology and Hepatology, Department of Internal Medicine, Keio University School of Medicine, Tokyo 1608582, Japan.

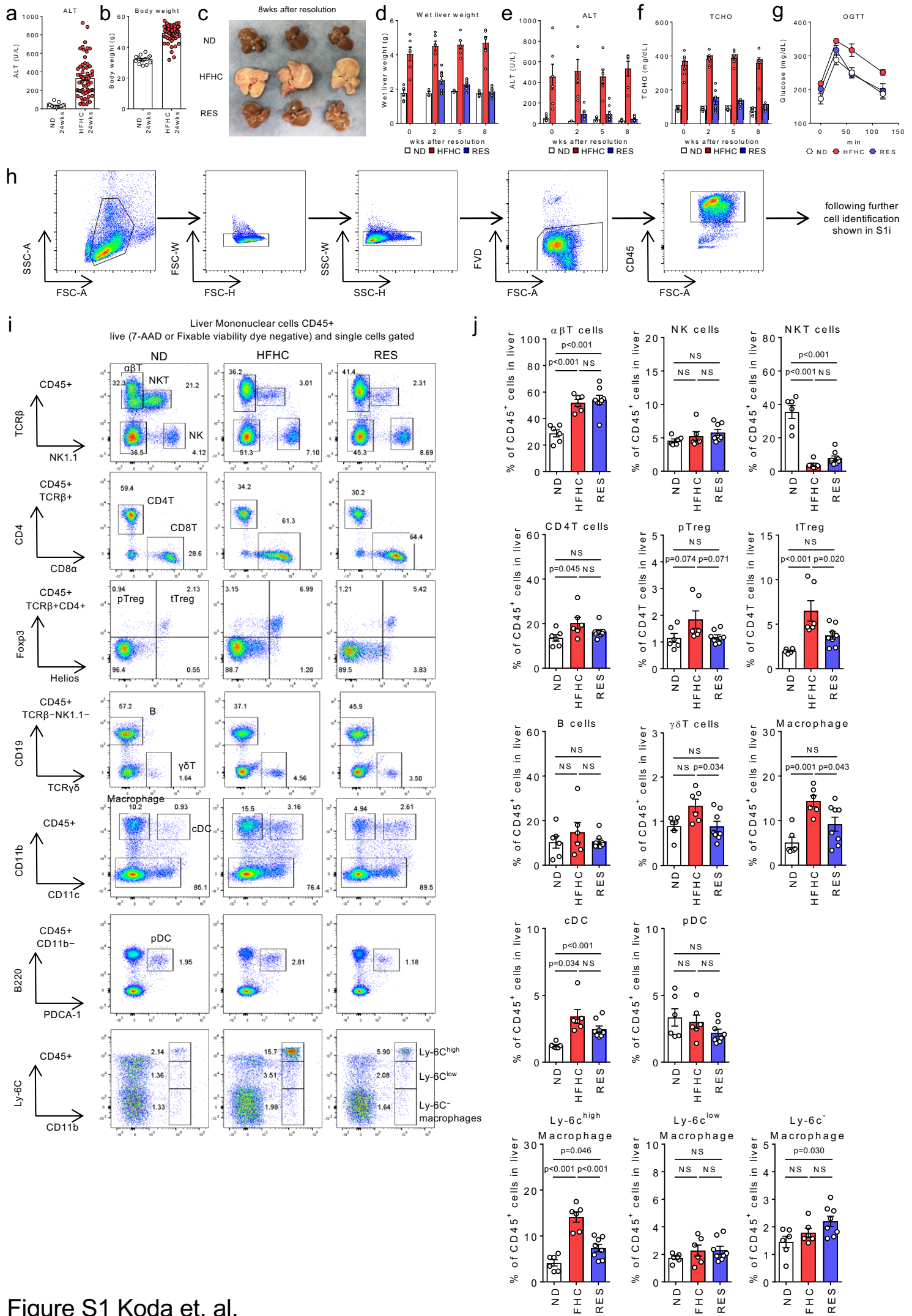
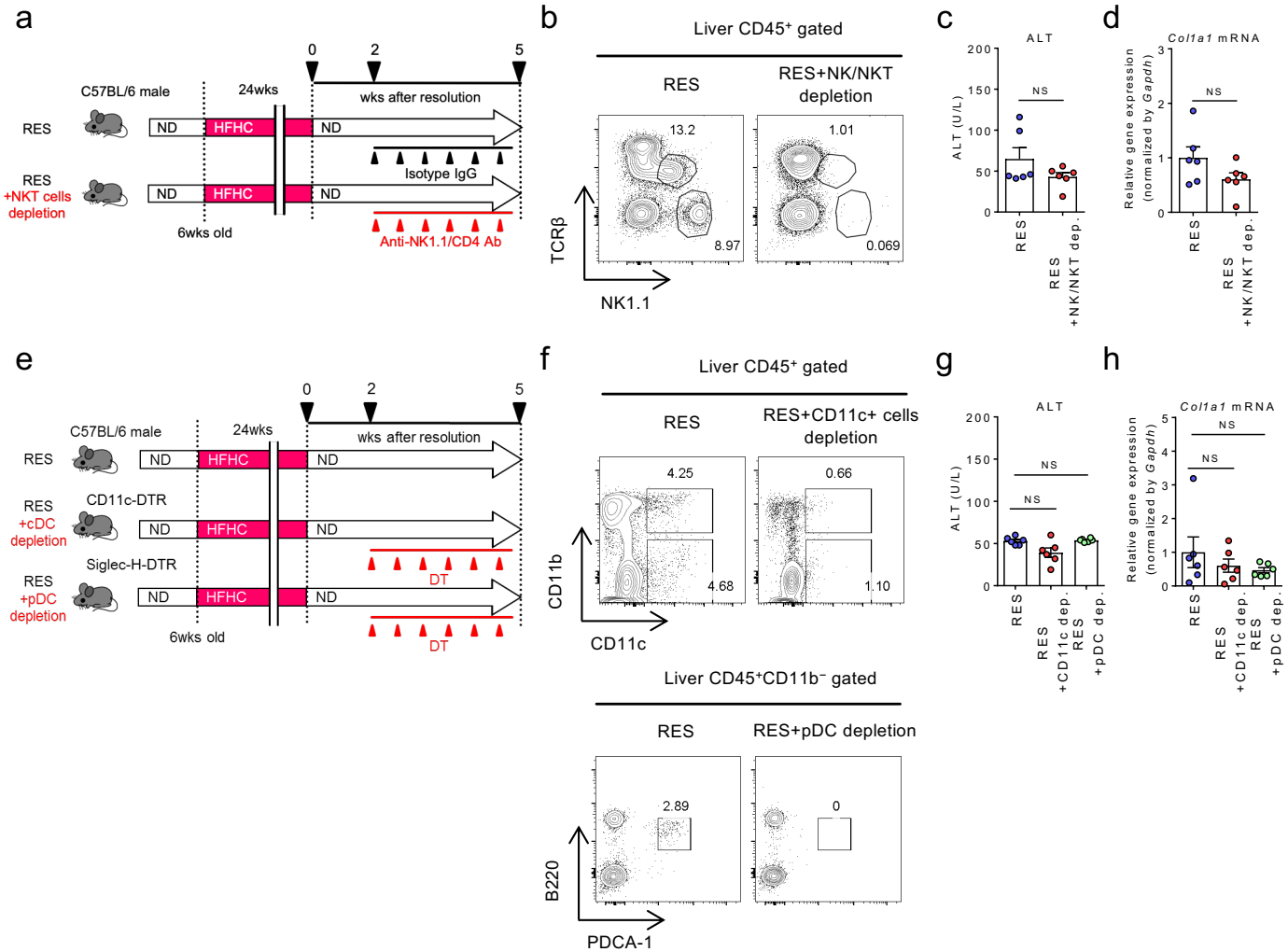
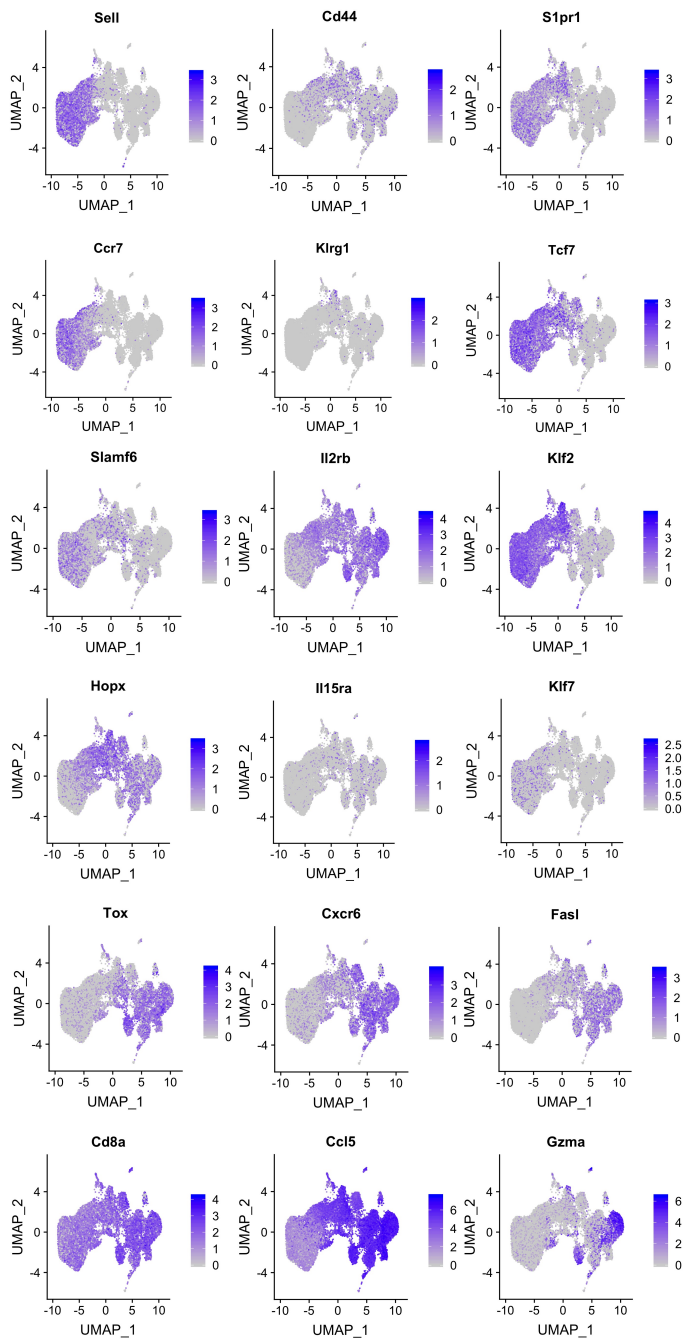


Figure S1 Koda et. al.

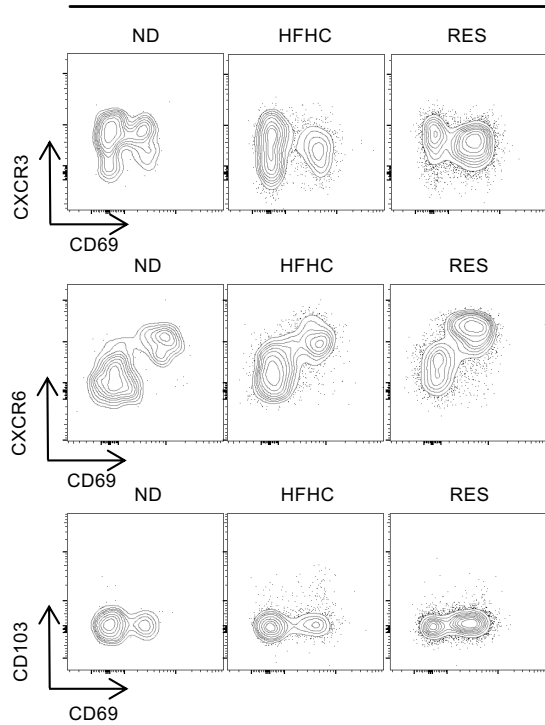
Supplementary Figure 1. Compensated data of HFHC-induced NASH and liver fibrosis resolution models. **a**, Serum ALT levels and **b**, body weight of HFHC-induced NASH mice (n=17 mice for ND 24 weeks group and n=63 mice for HFHC 24 weeks group). **c**, Representative gross photographs of livers. **d**, Wet liver weight, **e**, Serum ALT levels, **f**, Serum TCHO, and **g**, OGTT of ND, HFHC, and RES mice (**d-f**; n=3-6 mice for ND group, n=6 mice for HFHC group, and n=8 mice for RES group. **g**; n=4 mice for ND and RES groups, and n=3 mice for HFHC group). **h** and **i**, Gating strategy for FACS analysis. **j**, Frequency of the indicated immune cells in CD45⁺ liver MNCs (n= 6 mice for ND and HFHC groups, and n=8 mice for RES group). Data are presented as mean ± SEM. One-way ANOVA with Tukey's multiple comparisons post-hoc test was applied.



Supplementary Figure 2. CD11c⁺ myeloid cells, pDCs, NK cells, and NKT cells play no direct roles in NASH resolution. **a**, Study design: resolution induced mice were intraperitoneally treated with isotype control (RES group) or anti-NK1.1 antibody and anti-CD4 antibody (RES+NKT/NKT depletion group) once every three days for three weeks starting at week 2 following diet switch (n=6 mice per group). **b**, Representative TCR β /NK1.1 staining of CD45⁺ gated liver MNCs. **c**, Serum ALT levels. **d**, *Col1a1* mRNA levels. **e**, Study design: resolution induced mice (wild-type (WT), CD11c-DTR, or Siglec-H-DTR background) were either untreated or intraperitoneally treated with diphtheria toxin (DT) twice per week for three weeks starting at week 2 following diet switch (n = 6 mice per group). **f**, Representative TCR β /NK1.1 staining of CD45⁺ gated liver MNCs (upper) and B220/PDCA-1 staining of CD45⁺CD11b⁻ gated liver MNCs (lower). **g**, Serum ALT levels. **h**, *Col1a1* mRNA levels. Data are presented as mean \pm SEM. Two-sided unpaired Student's *t*-test (**c** and **d**) or one-way ANOVA with Tukey's multiple comparisons post-hoc test (**g** and **h**) was applied.



Supplementary Figure 3. Compensated data for scRNA-seq analysis of liver CD8⁺ T cells.
Expression levels of the specified marker genes on the UMAP plots of combined liver CD8⁺ T cells.



Supplementary Figure 4. Compensated data for FACS analysis of liver CD8⁺ T cells.
Representative CXCR3/CD69 (upper), CXCR6/CD69 staining (middle), and CD103/CD69 staining (lower) of CD45⁺TCR β ⁺NK1.1⁻CD8 α ⁺CD44⁺CD62L⁻ gated (Tem+Trm) liver MNCs derived from ND, HFHC, and RES (5 weeks) mice.

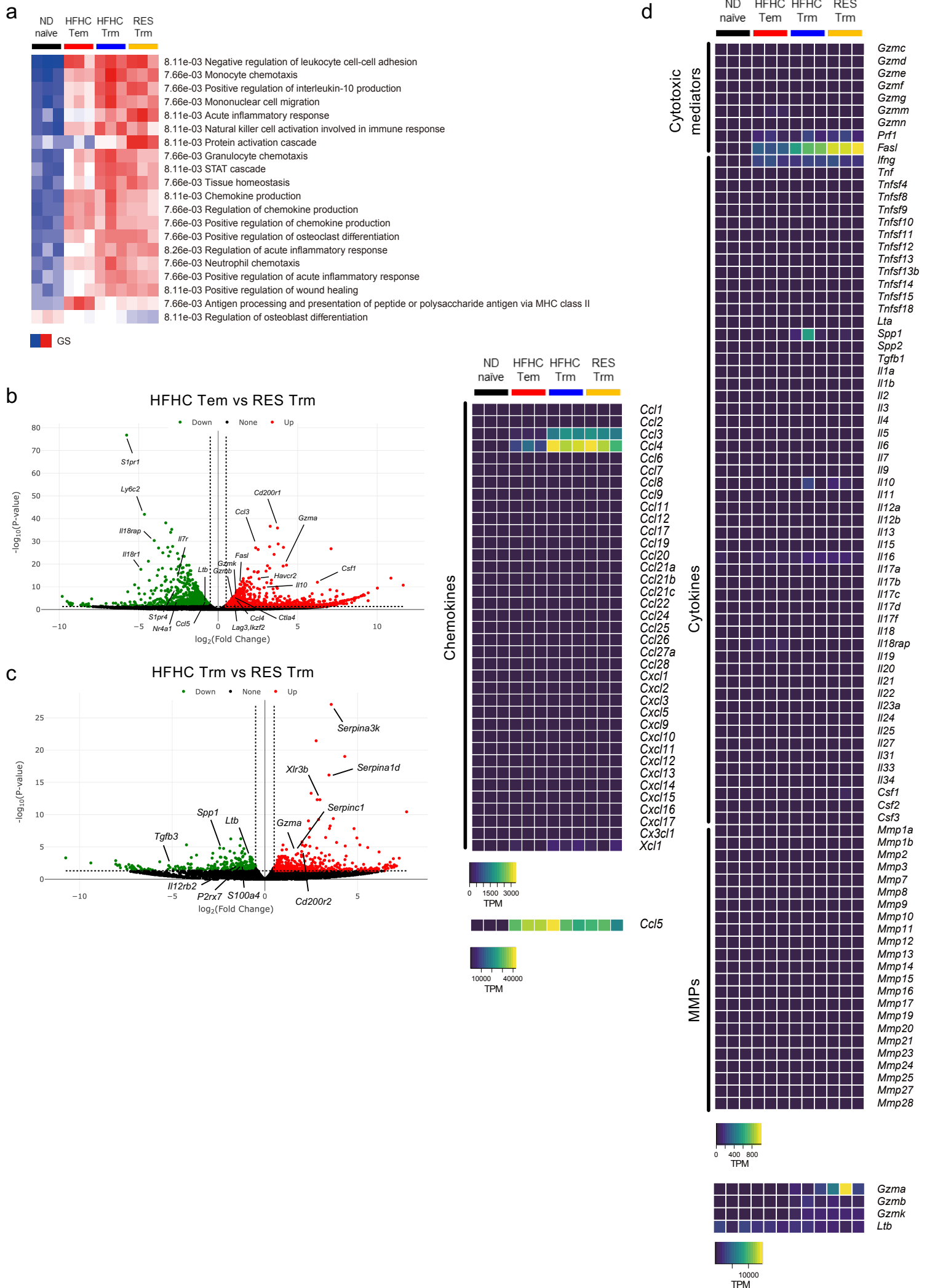
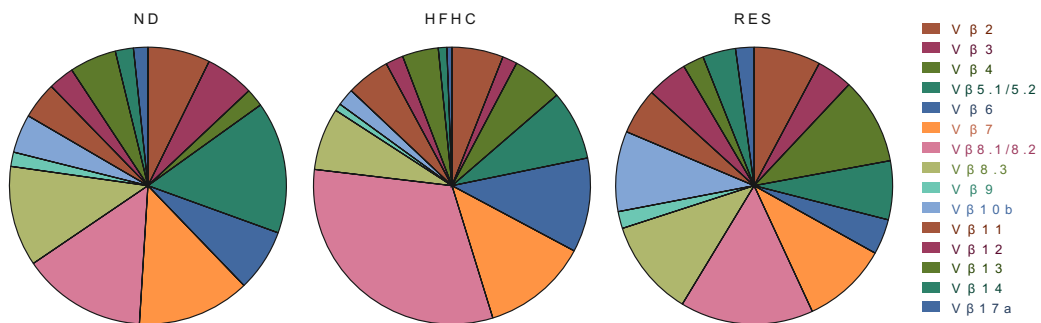
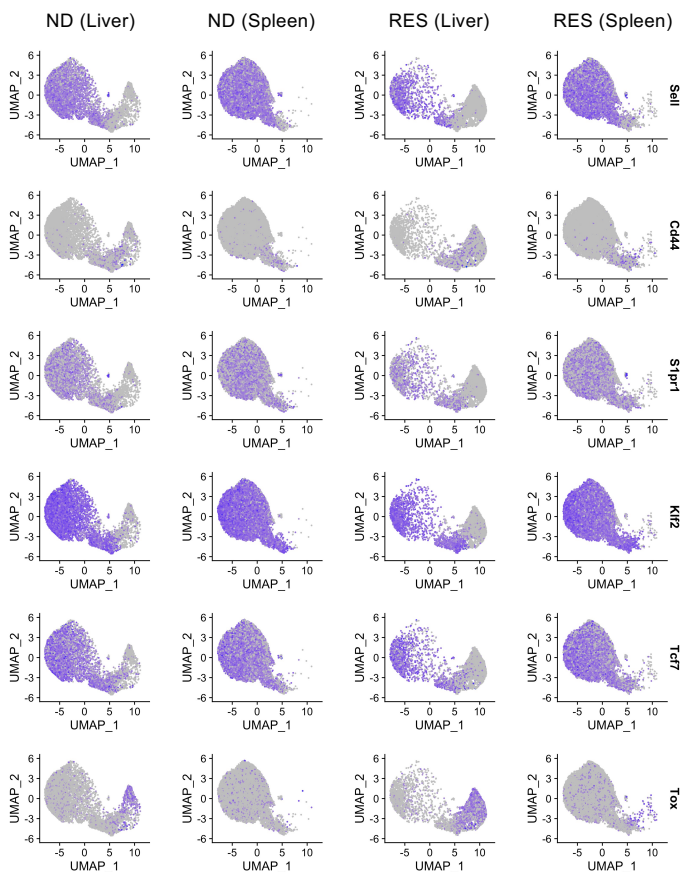


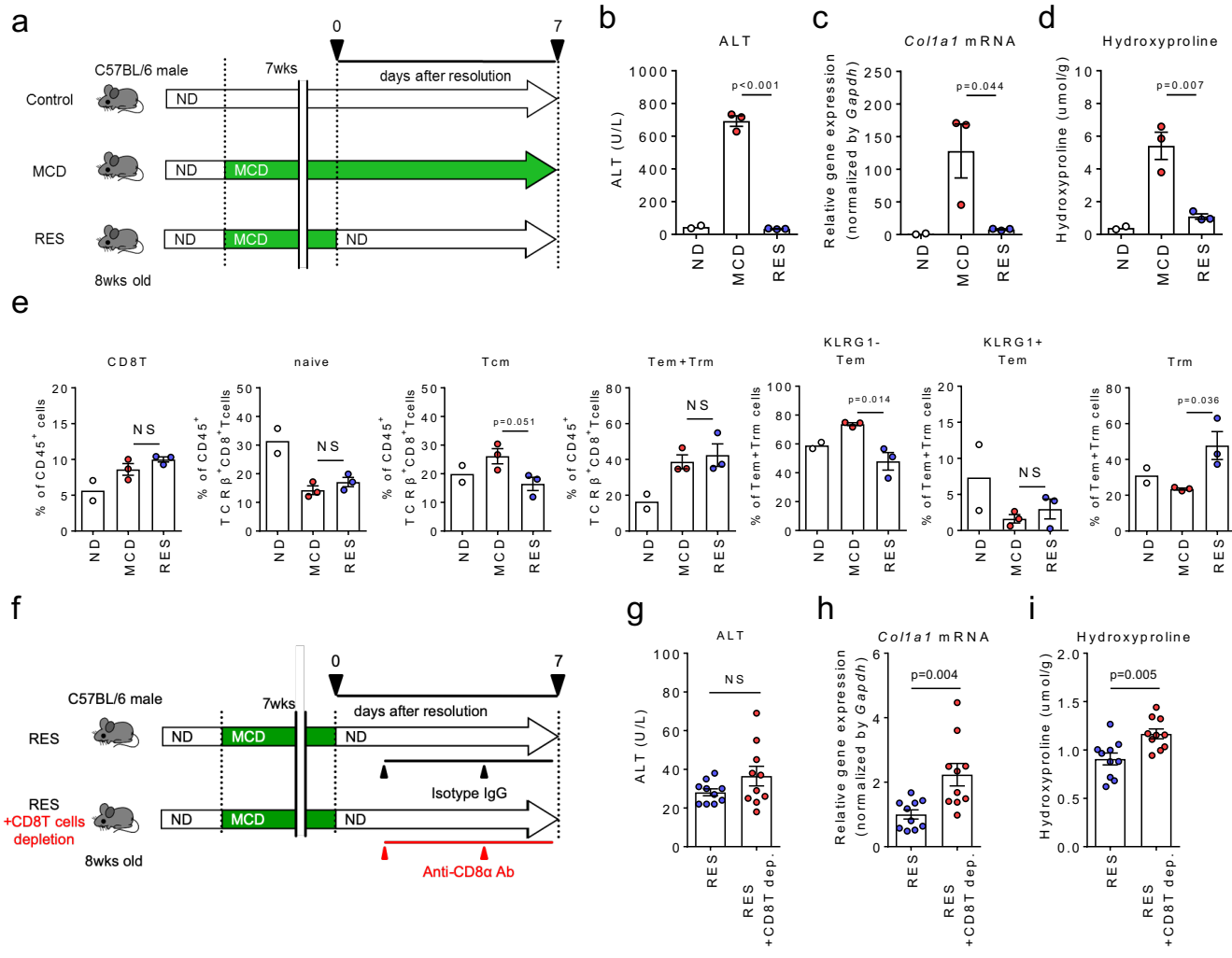
Figure S5 Koda et. al.

Supplementary Figure 5. Compensated data for bulk RNA-seq analysis of liver CD8⁺ T cells. **a**, Heat map from Gene ontology (GO) enrich analysis between the indicated groups. GO terms enriched in top 2000 significantly different genes were shown (top 20, FDR<0.1). **(b and c)** Volcano plot of HFHC Tem vs RES Trm (**b**), and of HFHC Trm vs RES Trm (**c**). Red and green dots mean significantly higher and lower genes in RES Trm ($P<0.01$, Fold change $>\log_21.5$), respectively. **d**, Heat map showing the absolute transcript levels of genes related to chemotaxis (left) and inflammatory pathways (right). Source data are provided as a Source data file.

a**b****c**

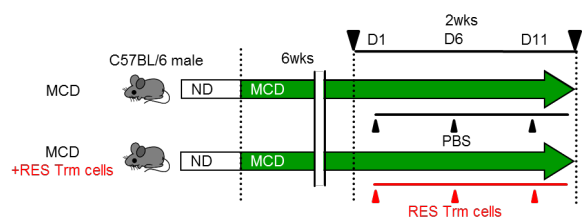
	ND (Liver)	ND (Spleen)	RES (Liver)	RES (Spleen)
clonotype1	4.81	0.08	39.94	0.26
clonotype2	0.98	0.05	9.06	0.19
clonotype4	0.55	0.04	3.46	0.10
clonotype3	0.45	0.04	3.40	0.16
clonotype5	0.61	0.03	2.89	0.07
clonotype6	0.42	0.04	1.74	0.07
clonotype7	0.54	0.04	1.35	0.05
clonotype8	0.33	0.03	1.31	0.06
clonotype9	0.30	0.02	1.08	0.06
clonotype10	0.21	0.02	1.00	0.04
Others	90.82	99.62	34.76	98.95

Supplementary Figure 6. TCR repertoire analysis of liver CD8⁺ Trm cells and compensated data for scTCR RNA-seq analysis of liver and spleen CD8⁺ T cells. **a**, Frequency of 15 different V β families in CD8⁺ Trm cells of ND, HFHC, and RES (5 weeks) mice (n=6 mice for ND and HFHC groups; n=8 mice for RES group) using FACS analysis. **b**, Expression levels of the specified marker genes on the UMAP plots in each cell subset. **c**, Percent values of each of the top 10 and other TCR clonotypes. Source data are provided as a Source data file.

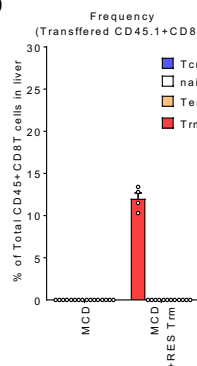


Supplementary Figure 7. CD8⁺ T cells play a direct role in MCD-induced liver fibrosis resolution. a, Study design: Male C57BL/6 mice were fed a ND or MCD diet for seven weeks, after which ND-treated mice were continuously fed a ND (ND group) for one week. MCD diet-treated mice were fed MCD diet (MCD group) or switched to ND (resolution; RES group) for one week to induce resolution (n=2 mice for ND group, and n=3 mice for MCD and RES groups). **b**, Serum ALT levels. **c**, *Col1a1* mRNA levels. **d**, Hydroxyproline levels. **e**, Proportion of each CD8⁺ T cell subset in CD45⁺ liver MNCs of the indicated groups. **f**, Study design: resolution induced mice were intraperitoneally treated with isotype control (RES group) or anti-CD8 α antibody (RES+CD8T depletion group) on day 1 and day 4 after the diet switch (n=10 mice per group). **g**, Serum ALT levels. **h**, *Col1a1* mRNA levels. **i**, Hydroxyproline levels. Data represent mean \pm SEM. Two-sided unpaired Student's *t*-test was applied (MCD vs. RES for **b-e**, and RES vs. RES+CD8T dep. for **g-i**).

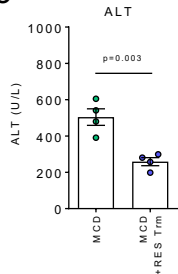
a



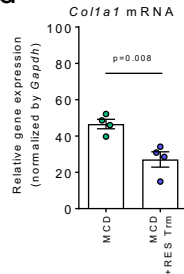
b



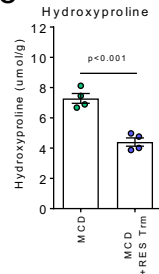
c



d

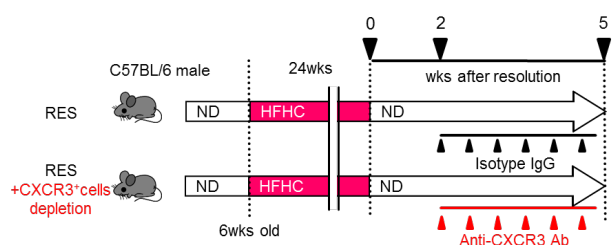


e

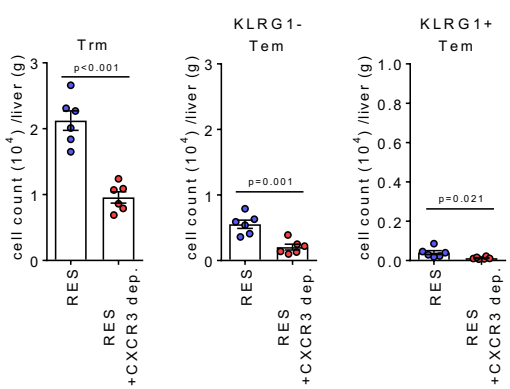


Supplementary Figure 8. Transfer of sorted CD8⁺ Trm cells ameliorates MCD-induced liver fibrosis. **a**, Study design: male C57BL/6 (Ly5.2) mice were fed a MCD diet for eight weeks and were intravenously injected with either PBS or liver CD8⁺ Trm (CD45⁺TCR β ⁺NK1.1⁻CD8 α ⁺CD44⁺CD62L⁻KLRG1⁻CD69⁺) cells isolated from Ly5.1RES (5 weeks) mice (2×10^6 cells each) on days 1, 6, and 11 starting at week six (n=4 mice per group). **b**, Frequency of the transferred CD8⁺ T cell subset in CD45⁺ liver MNCs of the indicated mice groups. **c**, Serum ALT levels. **d**, Col1a1 mRNA levels. **e**, Hydroxyproline levels. Data are presented as mean \pm SEM. Two-sided unpaired Student's *t*-test was applied.

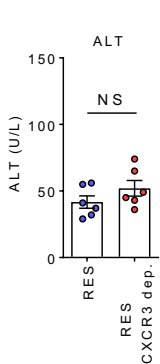
a



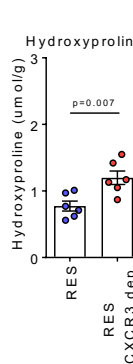
b



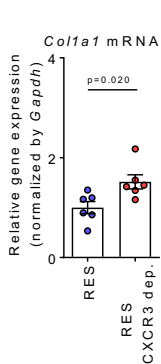
c



d

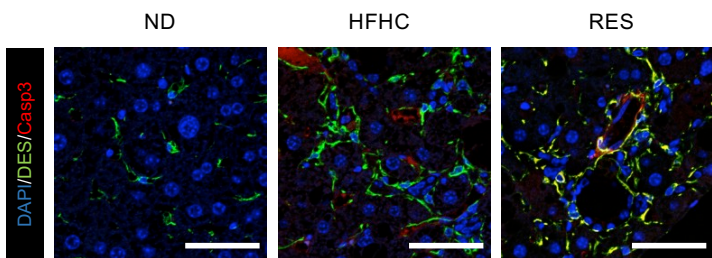


e

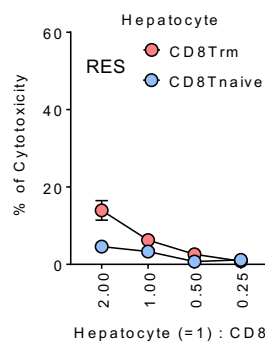


Supplementary Figure 9. Depletion of CXCR3⁺ cells prevents HFHC-induced liver fibrosis resolution. **a**, Study design: RES mice were treated with either anti-CXCR3 antibody (RES+CXCR3⁺ cells depletion group) or the isotype control (RES group) once every three days for three weeks starting at week 2 following diet switch (n=6 mice per group). **b**, Number of CD8⁺ Trm, KLRG1⁻ CD8⁺ Tem, and KLRG1⁺CD8⁺ Tem cells in CD45⁺ liver MNCs. **c**, Serum ALT levels. **d** Hydroxyproline levels. **e**, Col1a1 mRNA levels. Data are presented as mean \pm SEM. Two-sided unpaired Student's t-test was applied.

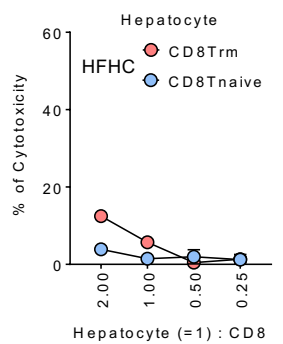
a



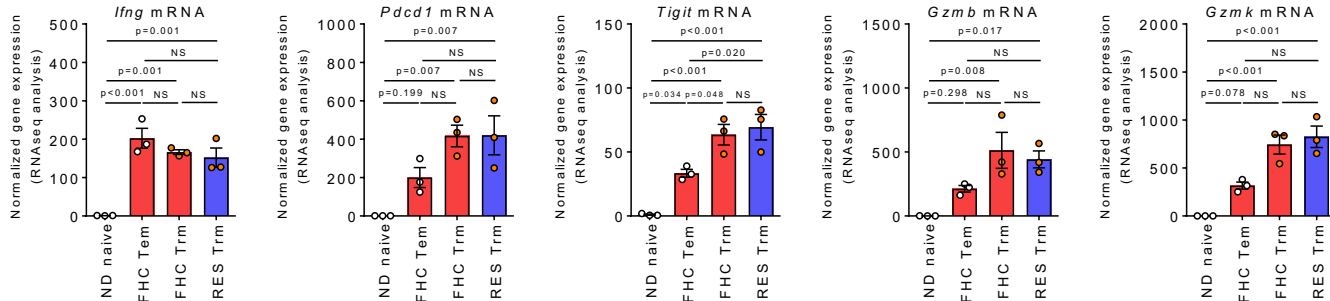
b



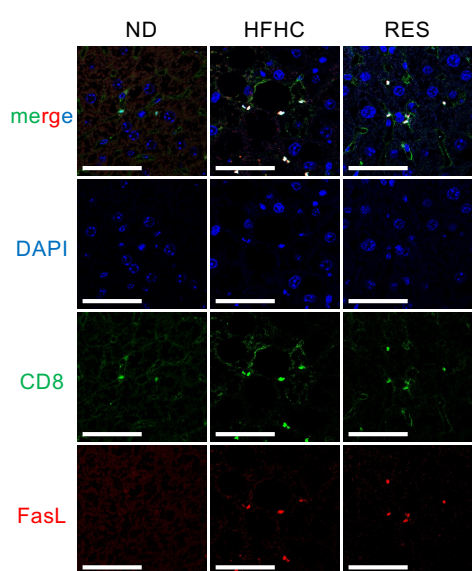
c



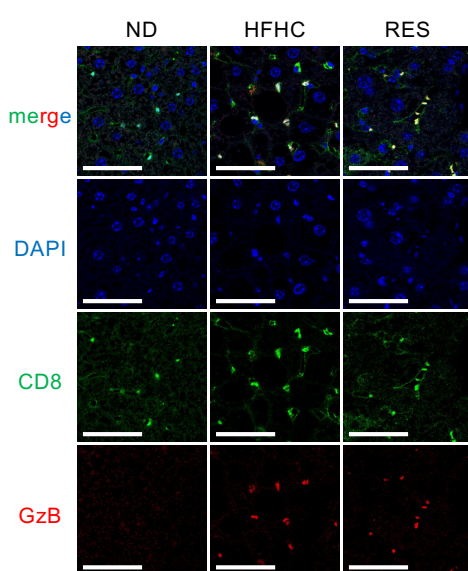
d



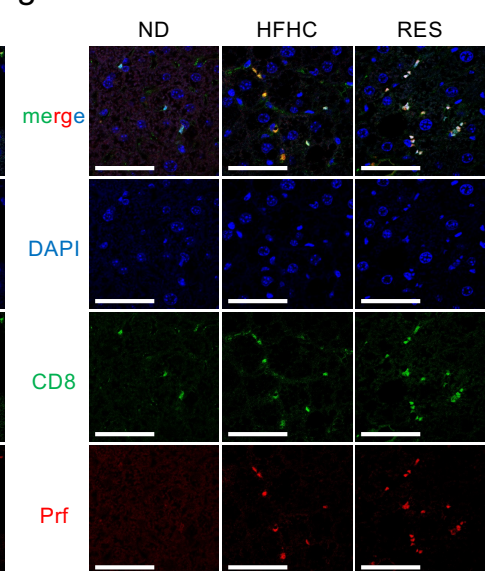
e



f



g



Supplementary Figure 10. Cytotoxicity of HSCs by CD8⁺ T cells. **a**, Representative photomicrographs of liver sections stained with DAPI (blue), anti-desmin (green), and anti-cleaved caspase 3 Ab (red). Scale bars: 50 µm. **b, c**, % cytotoxicity of hepatocytes by CD8 Trm (pink) or CD8 Tnaive (blue) isolated from RES 5 weeks mice (**b**) or HFHC mice (**c**) (n=3 biologically independent samples per group). **d**, *Ifng*, *Pdcd1*, *Tigit*, *Gzmb*, and *Gzmk* mRNA levels in ND naïve, HFHC Tem, HFHC Trm, and RES Trm cells (n=4 mice per group). Data are presented as mean ± SEM. One-way ANOVA with Tukey's multiple comparisons post-hoc test was applied. **e**, Representative fluorescent photomicrographs of liver sections stained with DAPI (blue), anti-CD8 Ab (green), and anti-FasL (red). Scale bars: 50 µm. **f**, Representative fluorescent photomicrographs of liver sections stained with DAPI (blue), anti-CD8 Ab (green), and anti-Granzyme B (Gzb) (red). Scale bars: 50 µm. **g**, Representative fluorescent photomicrographs of liver sections stained with DAPI (blue), anti-CD8 Ab (green), and anti-Perforin (Prf) (red). Scale bars: 50 µm. Photomicrograph data were representative from 4 independent samples and similar results were confirmed (**a, e-g**). Source data are provided as a Source data file.

Supplementary table 1. Clinical characteristics of participants

Background Characteristics	All participants	Normal	F1-2	F3-4
N	18	5	4	9
Sex, F: M	6:12	1:4	0:4	5:4
Age, yrs	70.5 [22-87]	48 [22-72]	72.5 [66-87]	75 [58-86]
AST, IU/L	36.5 [16-63]	20 [16-25]	43 [36-63]	43 [26-62]
ALT, IU/L	26.5 [10-84]	18 [10-25]	45 [20-84]	28 [14-64]
γ-GTP, IU/L	51.5 [14-163]	29 [14-127]	56.5 [45-84]	51 [21-163]
Platelet count, $\times 10^4/\mu\text{L}$	16.8 [6.3-22.6]	19.1 [18-22.6]	19.3 [16.6-22.4]	11.7 [6.3-19]
Total bilirubin, mg/dL	0.7 [0.4-2.4]	0.6 [0.4-1.3]	0.7 [0.6-1.0]	0.8 [0.4-2.4]
Serum albumin, g/dL	4.1 [3.0-4.6]	4.4 [4.3-4.6]	4.2 [4.1-4.2]	3.8 [3.0-4.2]
APRI	0.62 [0.19-2.34]	0.25 [0.19-0.34]	0.57 [0.53-0.70]	0.83 [0.51-2.34]
FIB-4 index	3.1 [0.54-11.0]	1.0 [0.54-1.94]	2.47 [2.04-4.12]	4.45 [2.37-11.0]

Data show median with ranges.

Supplementary table 2. List of antibodies used in this study

	antibody	Clonality	clone number	conjugate	Dilution	vendor	catalog number	Use
CD8	anti- mouse CD8 antibody	monoclonal	6A242		1/50	Santa Cruz Biotechnology	sc-70802	IHC
Desmin	anti- mouse desmin antibody	monoclonal			1/100	Abcam	ab15200	IHC
Desmin	anti- mouse desmin antibody	monoclonal	DE-U-10		1/100	Abcam	ab6322	IHC
cleaved caspase3	anti- mouse cleaved caspase Antibody	monoclonal	269518		1/100	R&D	MAB835	IHC
FasL	anti- mouse FasL antibody	polyclonal			1/100	sinobiological	101984	IHC
Fas	anti- mouse Fas antibody	polyclonal			1/100	R&D	AF435	IHC
Granzyme B	anti- mouse Granzyme B antibody	polyclonal			1/100	R&D	AF1865	IHC
Perforin 1	anti- mouse Perforin antibody	monoclonal	CB5.4		1/100	Abcam	ab16074	IHC
CD8	anti- human CD8 antibody	monoclonal	C8/144B		1/100	Nichirei	413211	IHC
CD69	anti- human CD69 antibody	monoclonal	EPR21814		1/100	Abcam	ab233396	IHC
	anti- rabbit IgG antibody (Secondary antibody)	polyclonal		Alexa Fluor 488		Abcam	ab150077	IHC
	anti- mouse IgG antibody (Secondary antibody)	polyclonal		Alexa Fluor 555		Abcam	ab150062	IHC
	anti- guinea pig IgG antibody (Secondary antibody)	polyclonal		Alexa Fluor 647		Abcam	ab150187	IHC
CD8α	anti- CD8α antibody	monoclonal	2.43			Bioxcell	BE0061	in vivo depletion
NK1.1	anti- NK1.1 antibody	monoclonal	PK136			Bioxcell	BE0036	in vivo depletion
CD4	anti- CD4 antibody	monoclonal	GK1.5			Bioxcell	BP0003-1	in vivo depletion
IL-15	anti- IL-15 antibody	monoclonal	A10.3			Bioxcell	BE0315	in vivo neutralization
FasL	anti- FasL antibody	monoclonal	MFL3			Bioxcell	BE0319	in vivo neutralization
CXCR3	anti- CXCR3 antibody	monoclonal	CXCR3-173			Bioxcell	BE0249	in vivo depletion
FasL	anti-1-FasL antibody	monoclonal	MFL4			BioLegend	106707	in vitro neutralization
IFN-γ	anti- IFN-γ antibody	monoclonal	XMG1.2			BD Biosciences	559065	in vitro neutralization
PD-1	anti- PD-1 antibody	monoclonal	29F.1A12			BioLegend	135246	in vitro neutralization
TIGIT	anti- TIGIT antibody	monoclonal	A17200C			BioLegend	622203	in vitro neutralization
CD45.2	anti- CD45.2 antibody	monoclonal	104	FITC	1/200	BD Biosciences	553772	FACS
CD45.2	anti- CD45.2 antibody	monoclonal	104	BV510	1/200	BD Biosciences	109838	FACS
CD45.1	anti- CD45.1 antibody	monoclonal	A20	FITC	1/200	BD Biosciences	553775	FACS
CD45.1	anti- CD45.1 antibody	monoclonal	A20	PE-Cy7	1/200	BioLegend	110729	FACS
CD45	anti- CD45 antibody	monoclonal	30-F11	BV510	1/200	BioLegend	103138	FACS
TCRβ	anti- TCR β chain antibody	monoclonal	H57-597	PerCP-Cy5.5	1/200	BD Biosciences	109228	FACS
TCRβ	anti- TCR β chain antibody	monoclonal	H57-597	APC	1/200	BD Biosciences	553174	FACS
TCRβ	anti- TCR β chain antibody	monoclonal	H57-597	APC-Cy7	1/200	BioLegend	109220	FACS
B220	anti- B220 antibody	monoclonal	RA3-6B2	PerCP-Cy5.5	1/200	BioLegend	103236	FACS
NK1.1	anti- NK-1.1 antibody	monoclonal	PK136	PE-Cy7	1/200	BioLegend	108714	FACS
CD4	anti- CD4 antibody	monoclonal	RM4-5	FITC	1/200	BD Biosciences	553047	FACS
CD4	anti- CD4 antibody	monoclonal	RM4-5	BV510	1/200	BD Biosciences	563106	FACS
CD8α	anti- CD8α antibody	monoclonal	53-6.7	FITC	1/200	BD Biosciences	553031	FACS
CD8α	anti- CD8α antibody	monoclonal	53-6.7	PerCP-Cy5.5	1/200	BD Biosciences	100734	FACS
CD8α	anti- CD8α antibody	monoclonal	53-6.7	APC	1/200	BD Biosciences	553035	FACS
CD8α	anti- CD8α antibody	monoclonal	53-6.7	APC-Cy7	1/200	BD Biosciences	557654	FACS
CD69	anti- CD69 antibody	monoclonal	H1.2F3	FITC	1/200	Thermo Fisher Scientific	11-0691-85	FACS
CD103	anti- CD103 antibody	monoclonal	2E7	BV421	1/200	BioLegend	121421	FACS
CXCR3	anti- CXCR3 antibody	monoclonal	CXCR3-173	APC	1/200	Thermo Fisher Scientific	17-1831-82	FACS
CXCR6	anti- CXCR6 antibody	monoclonal	SA051D1	APC	1/200	BioLegend	151105	FACS
CD62L	anti- CD62L antibody	monoclonal	MEL-14	PE	1/200	BD Biosciences	553151	FACS
KLRG1	anti- KLRG1 antibody	monoclonal	2F1/KLRG1	PerCP-Cy5.5	1/200	BioLegend	138417	FACS
CD44	anti- CD44 antibody	monoclonal	IM7	BV421	1/200	BioLegend	103039	FACS
CD11c	anti- CD11c antibody	monoclonal	HL3	FITC	1/200	BD Biosciences	557400	FACS
CD11c	anti- CD11c antibody	monoclonal	HL3	PE-Cy7	1/200	BD Biosciences	558079	FACS
Foxp3	anti- FOXP3 antibody	monoclonal	FJK-16s	PE	1/200	Thermo Fisher Scientific	12-5773-82	FACS
Foxp3	anti- FOXP3 antibody	monoclonal	FJK-16s	PerCP-Cy5.5	1/200	Thermo Fisher Scientific	45-5773-82	FACS
Helios	anti- Helios antibody	monoclonal	22F-6	APC	1/200	BioLegend	137222	FACS
TCRγδ	anti- TCR γδ chain antibody	monoclonal	GL3	PerCP-Cy5.5	1/200	BioLegend	118118	FACS
CD19	anti- CD19 antibody	monoclonal	1D3	PE	1/200	BD Biosciences	553786	FACS
CD11b	anti- CD11b antibody	monoclonal	M1/70	PE-Cy7	1/200	BD Biosciences	552850	FACS
CD11b	anti- CD11b antibody	monoclonal	M1/70	APC-Cy7	1/200	BD Biosciences	557657	FACS
PDCA-1	anti- PDCA-1 antibody	monoclonal	129c1	APC	1/200	BioLegend	127106	FACS
CCR5	anti- CCR5 antibody	monoclonal	7A4	PE	1/100	Thermo Fisher Scientific	12-1951-82	FACS
Mouse BD Fc Block	anti- CD16/CD32 antibody	monoclonal	2.4G2		1/100	BD Biosciences	553141	FACS
	Intracellular Fixation & Permeabilization Buffer Set					Thermo Fisher Scientific	88-8824-00	FACS
	Fixable Viability Dye eFluor 780				1/1000	Thermo Fisher Scientific	65-0865-14	FACS
	7-AAD Viability Staining Solution				1/100	BD Biosciences	51-68981E	FACS

Supplementary table 3. List of Taqman probes used in this study

Genes	catalog number	conjugate	vendor
<i>Col1a1</i>	Mm00801666_g1	FAM	Themo Fisher Scientific
<i>Col1a2</i>	Mm00483888_m1	FAM	Themo Fisher Scientific
<i>Acta2</i>	Mm00725412_s1	FAM	Themo Fisher Scientific
<i>Timp1</i>	Mm01341361_m1	FAM	Themo Fisher Scientific
<i>Desmin</i>	Mm00802455_m1	FAM	Themo Fisher Scientific
<i>Spp1</i>	Mm00436767_m1	FAM	Themo Fisher Scientific
<i>I115</i>	Mm00434210_m1	FAM	Themo Fisher Scientific
<i>Ccl3</i>	Mm00441258_m1	FAM	Themo Fisher Scientific
<i>Ccl4</i>	Mm00443111_m1	FAM	Themo Fisher Scientific
<i>Ccl5</i>	Mm01302427_m1	FAM	Themo Fisher Scientific
<i>Ccr5</i>	Mm001216171_m1	FAM	Themo Fisher Scientific
<i>Fas</i>	Mm00433237_m1	FAM	Themo Fisher Scientific
<i>Gapdh</i>	Mm99999915_g1	VIC	Themo Fisher Scientific